Supplementary information

Liquid-phase synthesis, sintering and transport properties of nanoparticle-based boron-rich composites

Guillaume Gouget,[a] Damien Bregiroux,[a] Rémi Grosjean,[a,b] David Montero,[c] Stefan Maier,[d] Franck Gascoin,[d] Clément Sanchez[a] and David Portehault[a,*]

[a] Sorbonne Université, CNRS, Collège de France, Laboratoire Chimie de la Matière Condensée de Paris, LCMCP, 4 Place Jussieu, F-75005 Paris, France.
[b] Sorbonne Université, CNRS, MNHN, IRD, Institut de Minéralogie, de Physique des Matériaux et de Cosmochimie, IMPMC, 4 Place Jussieu, F-75005 Paris, France.
[c] Sorbonne Université, CNRS, Institut des Matériaux de Paris Centre, IMPC, 4 place Jussieu, F-75005 Paris, France.
[d] Laboratoire CRISMAT UMR 6508 CNRS ENSICAEN, 6 boulevard du Maréchal Juin, 14050 Caen Cedex 04, France.

*Corresponding author: david.portehault@sorbonne-universite.fr

Table S1. Masses of precursors and LiCl/KCl (45/55 wt %) for syntheses with various hafnium-to-boron molar ratios (Hf:B).

Hf:B	m($HfCl_4$) (mg)	m($NaBH_4$) (mg)	m(LiCl/KCl) (g)
1:3	641	227	5.00
1:3.5	641	132	5.00
1:4	641	303	5.00
1:5	641	378	5.00
1:6	641	454	5.00
1:8	320	303	2.50
1:12	320	454	2.50

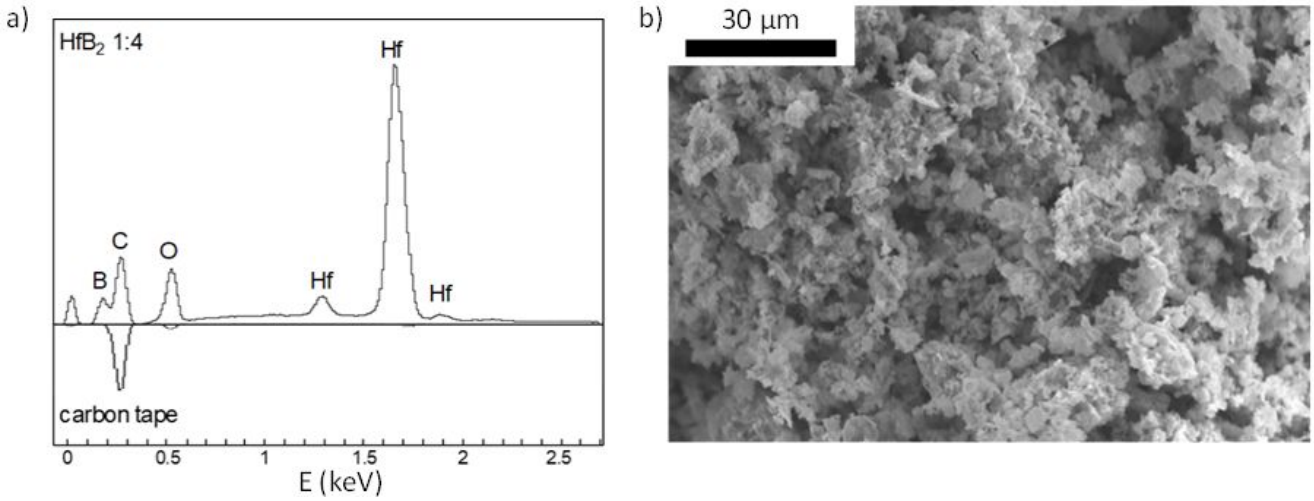

Figure S1. a) SEM-EDS spectrum of the nanocomposite with an initial hafnium-to-boron ratio of 1:4 and carbon tape only. Both samples were covered with a thin layer of carbon by evaporation. The spectra are normalized to carbon contribution and the carbon tape diagram is inverted for comparison. b) SEM picture of a region used for EDS measurement on HfB_2 1:4 sample. At 10 kV acceleration voltage, the depth of X-ray generation calculated by the Anderson-Hasler formula is about 713 nm for boron in $Hf_{0.2}B_{0.6}O_{0.2}$ ($d_{1:4}$ = 6.81 g.cm^{-3}), assuming a homogeneous composition of the material. The powder deposited was thick enough for analysis in sheer volume at 10 kV.

Table S2. Cell parameters of HfB_2 from (a) ICDS card 30422 and (b) Le Bail refinements of nanocomposites for initial hafnium-to-boron molar ratios ranging from 1:3 to 1:12. Deviations from the reference are also displayed. The cell parameters deviate more with increased initial boron introduced: *a* = *b* increases, while *c* decreases, which corresponds to boron hexagonal sheets coming closer one to each other in the lamellar structure of HfB_2. For samples 1:8 and 1:12, the parameter cell *a* is overestimated in LeBail refinements compared to experimental diagrams (**Figure 2**). This is related to the very broad peaks complicating background fitting.

a

Reference	a = b (Å)	c (Å)
ICSD 30422	3.141(2)	3.470(2)

b

Sample	a = b (Å)	Δa (%)	c (Å)	Δc (%)	Rp (%)	wRp (%)
1:3	3.1424(1)	0.04	3.4745(2)	0.13	0.98	1.53
1:3.5	3.1430(4)	0.06	3.4742(2)	0.12	0.63	0.83
1:4	3.1457(4)	0.15	3.4732(6)	0.09	0.89	1.44
1:5	3.1474(3)	0.20	3.4708(3)	0.02	0.48	0.60
1:6	3.1460(4)	0.16	3.4726(6)	0.07	0.52	0.65
1:8	3.1573(5)	0.52	3.4684(6)	0.05	0.33	0.43
1:12	3.1505(8)	0.30	3.4614(9)	0.25	0.42	0.55

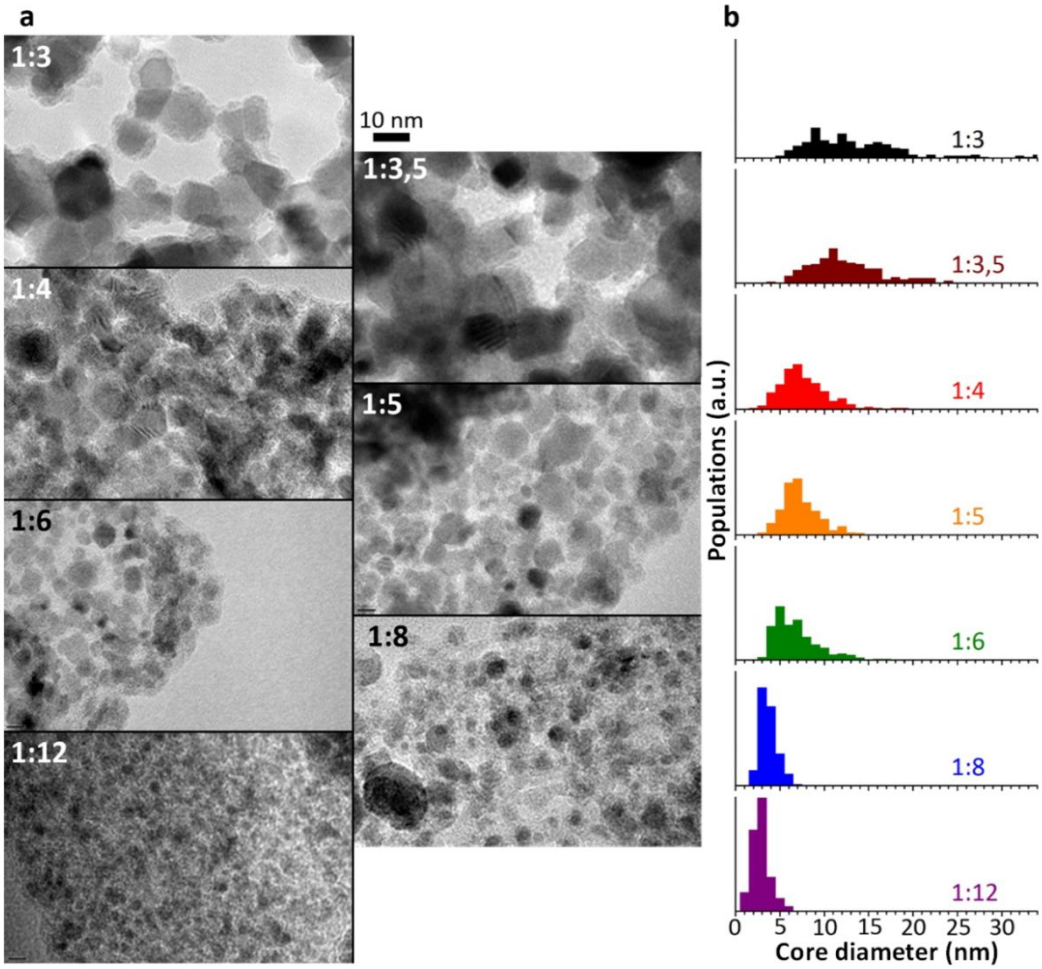

Figure S2. a) TEM micrographs and b) size distribution diagrams of HfB_2 nanocrystals for initial hafnium-to-boron molar ratios ranging from 1:3 to 1:12. Size distributions are plotted out of at least 200 particle counts. Data for ratios 1:4 to 1:12 are taken from ref. 32. Reproduced from reference 32. Copyright 2018 American Chemical Society

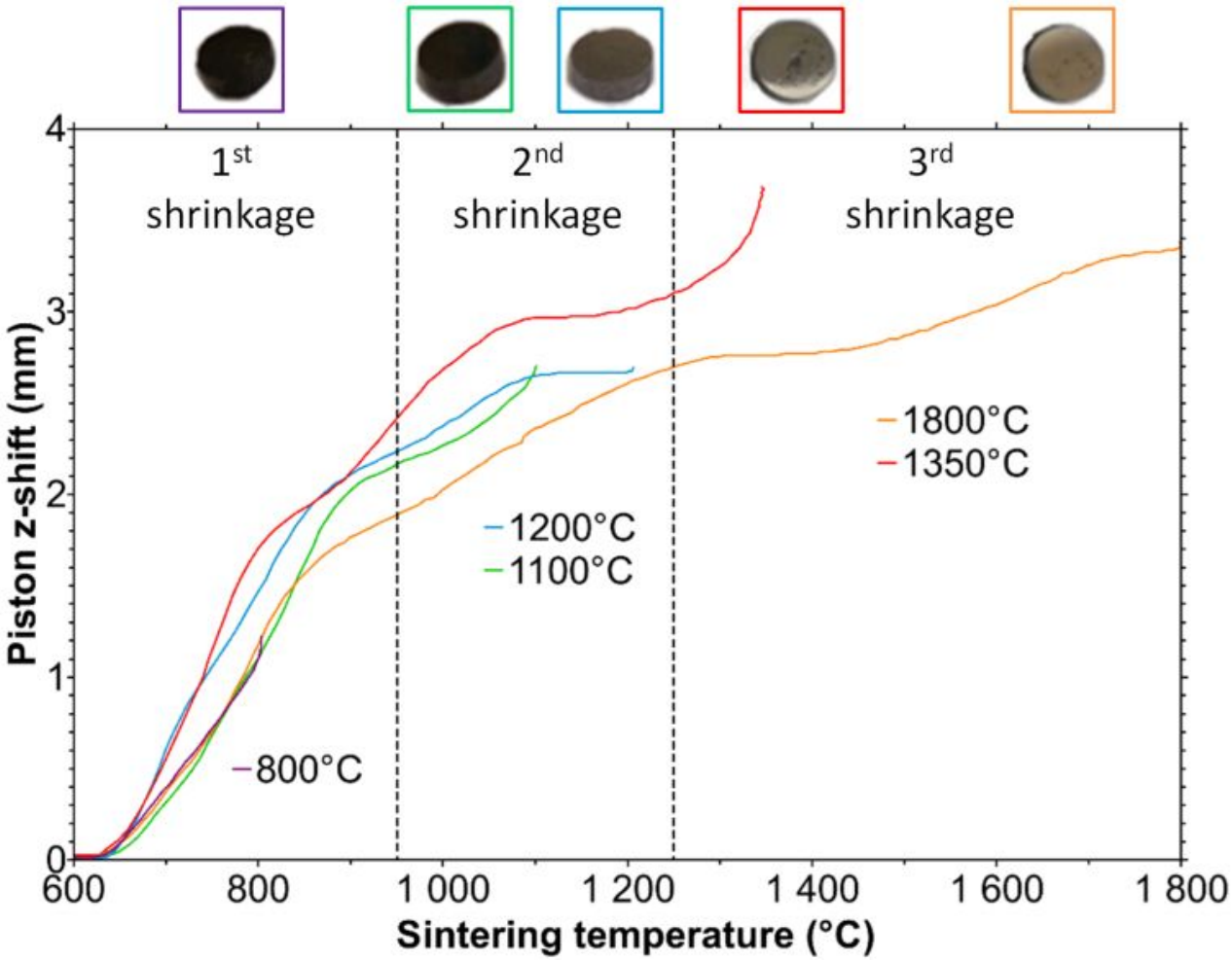

Figure S3. Piston uniaxial shift along z coordinate as a function of temperature. The z-shift value is relative to the pistons position after the temperature measured by the pyrometer is stabilized at 600 °C. As temperature increases, three shrinkages of the sample can be distinguished when temperature above approx. 1250 °C is reached. They occur at distinct temperature ranges. Samples sintered between 950 and 1250 °C undergo two shrinkages, while below 950 °, only the first shrinkage is observed.

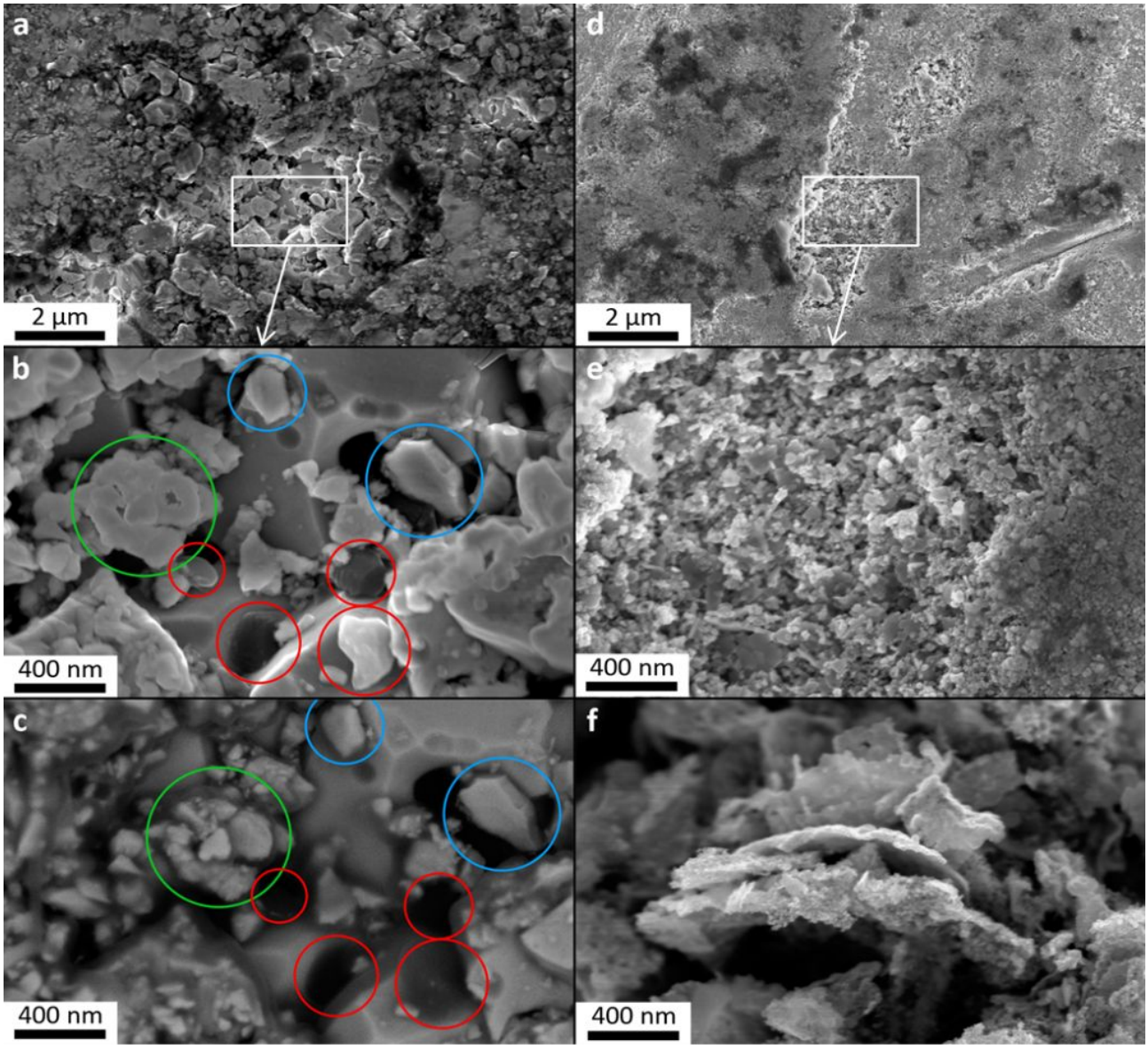

Figure S4. SEM-FEG micrographs of pellets sintered under 100 MPa at (a-c) 1800 and (d,e) 1100 °C, from (f) the powder with an initial Hf:B molar ratio of 1:4. (a,d) A rough polishing step yields surfaces displaying homogeneously contrasted regions of dense aggregates that are extended compared to the particles grain size. In addition, scratched out surfaces allow to detect packed particles within the composite, as observed in (b,c) and (e). (b) and (c) pictures depict the same region through collection of secondary and back-scattered electrons, respectively. The latter technique is sensitive to electron density, leading to a Z-sensitive contrast (all other images are acquired in secondary electron image mode). Here, faceted particles such as those circled in blue remain bright upon back-scattered electrons, which is attributed to the occurrence of hafnium in HfB_2 particles. On the contrary, particles circled in red are darkened during the acquisition of back-scattered electrons. These particles are poorly faceted, not concentrated in Hf, therefore they are assigned to boron-rich particles. Note that some particles or aggregates keep the initial core-shell structure with core diameters ranging from approx. 20 to 200 nm (circled in green). (e) After SPS at 1100 °C (d-e), the pellet is composed of nanoparticles homogeneous in contrast and size of about 10-20 nm, though slightly bigger than in (f) the initial powder of aggregated nanoparticles.

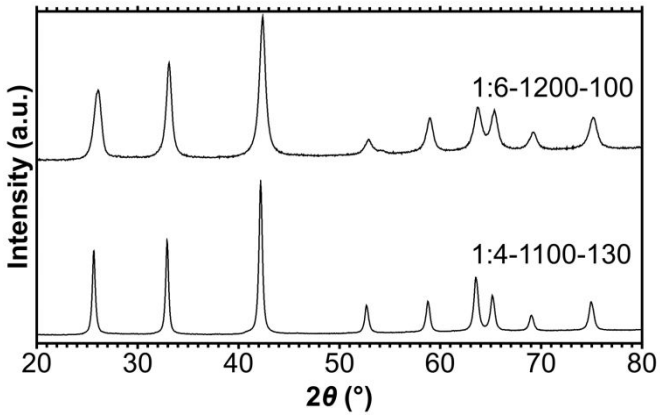

Figure S5. XRD diagrams of the pellets obtained from (i) an initial hafnium-to-boron molar ratio Hf:B of 1:6 followed by spark plasma sintering at 1200 °C and 100 MPa (1:6-1200-100), and (ii) Hf:B of 1:4 and SPS at 1100 °C and 130 MPa.

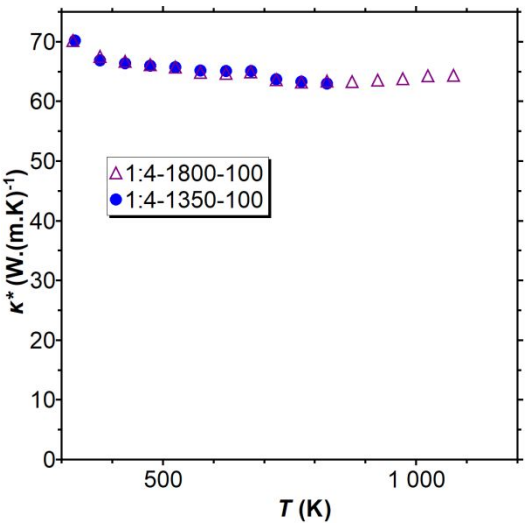

Figure S6. Thermal conductivities in boron-rich dense nanocomposites (Hf:B-T (°C)-P (MPa)).